Demyelinating and Nondemyelinating Strains of Mouse Hepatitis Virus Differ in Their Neural Cell Tropism[▽]

Jayasri Das Sarma,[1]* Kathryn Iacono,[2]† Lilli Gard,[2]‡ Ryan Marek,[1] Lawrence C. Kenyon,[3] Michael Koval,[4] and Susan R. Weiss[2]

Department of Neurology, Thomas Jefferson University, Philadelphia, Pennsylvania 19107[1]; Department of Microbiology, University of Pennsylvania, Philadelphia, Pennsylvania 19104[2]; Department of Pathology, Anatomy and Cell Biology, Thomas Jefferson University, Philadelphia, Pennsylvania 19107[3]; and Pulmonary, Allergy, and Critical Care Medicine Division, Department of Medicine, Emory University, Atlanta, Georgia 30322[4]

Some strains of mouse hepatitis virus (MHV) can induce chronic inflammatory demyelination in mice that mimics certain pathological features of multiple sclerosis. We have examined neural cell tropism of demyelinating and nondemyelinating strains of MHV in order to determine whether central nervous system (CNS) cell tropism plays a role in demyelination. Previous studies demonstrated that recombinant MHV strains, isogenic other than for the spike gene, differ in the extent of neurovirulence and the ability to induce demyelination. Here we demonstrate that these strains also differ in their abilities to infect a particular cell type(s) in the brain. Furthermore, there is a correlation between the differential localization of viral antigen in spinal cord gray matter and that in white matter during acute infection and the ability to induce demyelination later on. Viral antigen from demyelinating strains is detected initially in both gray and white matter, with subsequent localization to white matter of the spinal cord, whereas viral antigen localization of nondemyelinating strains is restricted mainly to gray matter. This observation suggests that the localization of viral antigen to white matter during the acute stage of infection is essential for the induction of chronic demyelination. Overall, these observations suggest that isogenic demyelinating and nondemyelinating strains of MHV, differing in the spike protein expressed, infect neurons and glial cells in different proportions and that differential tropism to a particular CNS cell type may play a significant role in mediating the onset and mechanisms of demyelination.

Multiple sclerosis is a common disabling neurological disease, pathologically characterized by demyelination, loss of oligodendroglial cells, and axonal degeneration (25, 26). The mechanisms that culminate in the destruction of oligodendrocytes and loss of central nervous system (CNS) myelin are not well understood. The process is believed to involve a T-cell-mediated autoimmune phenomenon that may be triggered by one or more viral infections (1). Several experimental viral model systems have been instrumental in providing these insights (2). One of the animal models is based on mouse hepatitis virus (MHV)-induced demyelination in mice that mimics the pathology of multiple sclerosis (12, 19, 21, 39, 42). Infection with neurotropic MHV strains produces a biphasic neurological disease, with acute meningoencephalitis preceding the onset of chronic demyelination (21).

Following intracranial inoculation, MHV is first observed in the brain and subsequently spreads into the spinal cord (30). The viral titer reaches its peak at approximately day 5 postinfection. Infectious viral particles are cleared within the first 7 to 10 days after infection, although viral RNA persists in the white matter of the spinal cord for several months (20, 29). Viral RNA persistence has previously been demonstrated in spinal cords of mice infected with demyelinating strains of MHV, including MHV-A59 and JHM (17, 20, 29), and has previously been suggested to be a prerequisite for MHV-induced demyelination. Indeed, MHV-2 and Penn 97-1 (a nondemyelinating recombinant strain of MHV) (3), which do not persist, also do not cause demyelination (4). Interestingly, the viral RNA of SMHV2-RA59, a chimeric strain (a nondemyelinating strain of MHV, expressing MHV-2 spike gene in the MHV-A59 background, previously called Penn 98-1/2), persists in the spinal cord during chronic infection and, yet, is unable to induce demyelination (4), indicating that viral RNA persistence in the spinal cord per se is insufficient to induce chronic demyelination. If exchanged between strains, genes for the spike protein, which are known to mediate viral entry, may alter the capacity of MHV to infect and replicate in particular CNS cell types (neurons, astrocytes, microglia, and oligodendrocytes) during the acute stage of infection, and therefore influence the induction of chronic demyelination.

Little is known about the involvement of CNS cell tropism in MHV-induced demyelination. It is known, however, that in the CNS, demyelinating MHVs infect a variety of neural cell types, including neurons, astrocytes, oligodendrocytes, microglia, and ependymal cells (15, 19, 21, 43). Recently, by using JHM spike chimeric viruses, Phillips et al. (32) demonstrated that spike gene-mediated neurovirulence of MHV is associated with extensive viral spread in the brain in both neurons and astrocytes.

However, no studies have examined whether nondemyelinating MHV strains infect the same CNS cell types as do demyelinating strains.

We have examined CNS cell tropism of both demyelinating and nondemyelinating MHV strains during the acute stage of infection in order to determine how the infection of a particular cell type(s) influences the likelihood of development of chronic demyelination. This examination entailed asking whether nondemyelinating strains differ in their abilities to infect gray and white matter cells in the spinal cord during acute infection.

We used the recombinant MHVs SJHM-RA59$_{EGFP}$ (highly neurovirulent and demyelinating), RA59$_{EGFP}$ (weakly neurovirulent but demyelinating) (38), and SMHV2-RA59$_{EGFP}$ (neurotropic but nondemyelinating) (33). All three viruses express enhanced green fluorescent protein (EGFP) and are isogenic, except for the spike gene, and differ in their neurovirulence and demyelination properties.

During acute infection, these three isogenic recombinant MHVs differ in spread and also in their CNS cell tropism. Most interestingly, viral antigen of the demyelinating strains is first detected in gray matter, with subsequent localization to white matter; while antigen of nondemyelinating strains is restricted mainly to gray matter, with occasional distribution to white matter. The distribution of viral antigen in white matter during the acute stage of infection may be one of the key factors in chronic viral persistence and induction of demyelination.

MATERIALS AND METHODS

Viruses and cells. EGFP-expressing recombinant viruses SJHM-RA59$_{EGFP}$ and RA59$_{EGFP}$ are isogenic, except that SJHM-RA59$_{EGFP}$ expresses the JHM spike gene and RA59$_{EGFP}$ carries the MHV-A59 spike gene (38). These two EGFP-expressing viruses were generated from our previous studies (38), where they were named S$_{JHM}$-R$_{EGFP}$ and S$_{A59}$-R$_{EGFP}$ for SJHM-RA59$_{EGFP}$ and RA59$_{EGFP}$, respectively.

Construction of SMHV2-RA59$_{EGFP}$. To construct the nondemyelinating, EGFP-tagged, isogenic, recombinant strain SMHV2-RA59$_{EGFP}$, the MHV-2 (a nondemyelinating MHV strain) (3) spike gene was cleaved from pMH54-SMHV2$_{EGFP}$ with AvrII and SbfI restriction digestion and inserted into the pMH54$_{EGFP}$ in place of the A59 spike gene (4). Targeted RNA recombination was carried out as described in our previously published work (38). For each desired recombinant, at least two strains derived from independent recombination events were characterized. EGFP-expressing viruses with the MHV-2 spike gene were labeled SMHV2-RA59$_{EGFP}$. We previously used this recombinant EGFP-tagged strain of SMHV2-RA59 in our other studies (33).

Inoculation of mice. Four-week-old, MHV-free C57BL/6 (B6) male mice (National Cancer Institute, Frederick, MD) were used in all experiments. Mice were anesthetized with isoflurane (IsoFlo; Abbott Laboratories, North Chicago, IL) prior to inoculation. For intracranial inoculations, 20 μl of diluted virus (in phosphate-buffered saline [PBS] containing 0.75% bovine serum albumin) was injected into the left cerebral hemisphere. Mock-infected controls were inoculated in a manner similar to that described above, but with an uninfected 17Cl-1 cell lysate at a comparable dilution. All experimental procedures were approved by the Institutional Animal Care and Use Committee.

Virulence and viral titers in mice. Virulence was assayed by calculating the 50% lethal dose (LD$_{50}$). Mice were inoculated intracranially with 10-fold serial dilutions of viruses (five mice per dilution). Signs of disease or death were monitored on a daily basis for up to 30 days postinfection. LD$_{50}$ values were calculated by the method of Reed and Muench (34). For measurement of viral titers in the liver and the brain, mice were sacrificed at 1, 3, 5, 7, 9, and 11 days postinfection and perfused with 2 ml of sterile PBS. Brains and livers were removed aseptically and placed separately and directly into 5 ml of isotonic saline with 0.167% gelatin (gel saline). All organs were weighed and stored frozen at −80°C. Brains and livers were homogenized, and viral titers were determined by plaque assay on L2 cell monolayers (4).

Histopathological analysis. For analysis of organ pathology, mice were infected intracranially, sacrificed at various times (days 3, 5, 7, and 10 postinfection), and perfused with 5 ml of saline, followed by 10% phosphate-buffered formalin. Brains and spinal cords were removed, and tissues were embedded in paraffin and sectioned for staining. Brain and spinal cord sections were stained with hematoxylin and eosin (H&E) and used for pathological evaluations by light microscopy. For an assessment of demyelination, mice were inoculated intracranially with half of an LD$_{50}$ (0.5LD$_{50}$) dose (eight mice per virus strain) and sacrificed at day 30 postinfection. Spinal cord sections were stained with Luxol fast blue to detect plaques of demyelination. We repeated the demyelination experiment five times, with eight mice in each group. Demyelination was quantified by examining four quadrants from two different levels of spinal cord sections for each mouse; thus, approximately 80 quadrants were examined for each virus. All slides were coded and read in a blinded fashion (4).

Immunohistochemical analysis. Immunohistochemical analysis was performed by the avidin-biotin-immunoperoxidase technique (Vector Laboratories, Burlington, CA) using 3,3′ diaminobenzidine as the substrate and a 1:20 dilution of monoclonal antibody directed against the nucleocapsid protein (N) of MHV-JHM (monoclonal antibody clone 1-16-1 [kindly provided by Julian Leibowitz]). Control slides from mock-infected mice were incubated in parallel. All slides were read in a blinded manner.

Immunofluorescence. Mice were inoculated intracranially and sacrificed (five mice per group) at days 3, 5, and 7 postinfection. Infected mice were perfused transcardially with PBS, followed by cold PBS containing 4% paraformaldehyde and finally with 10 ml of PBS containing 10% sucrose. Brains were removed and placed at 4°C for 4 h in 10% sucrose, followed by 30% sucrose overnight. Tissues were embedded in OCT medium (Tissue Tek, Hatfield, PA), sectioned sagitally with a microtome to 6-μm thickness, and mounted on glass slides. Some sections were stained with H&E, while others were left unstained for EGFP detection and immunofluorescence. To detect EGFP fluorescence without immunostaining, frozen brain sections were fixed in ice-cold 95% ethanol for 20 min, incubated at room temperature in ice-cold PBS for 10 min, and then mounted in 4.8% Mowiol in 50% glycerol. Sections were visualized using an Olympus X-70 microscope system with a 10× long-working-distance UPlanF1 phase objective and a filter pack suitable for green fluorescence (U-MWIBA; exciter, BP460-490; beam splitter, DM505; emitter, BA515-550). We repeated the acute-stage cell tropism experiment with five mice in each group at a 0.5LD$_{50}$ dose and repeated the experiment three times. We also infected groups of five mice at 500 PFU and 1,000 PFU and obtained similar results in terms of cellular tropism. This experiment was repeated twice.

Double-label immunofluorescence. Frozen tissue sections were washed with PBS at room temperature in a humidified chamber, incubated for 10 min at room temperature with 1 mg/ml NaBH$_4$ in PBS to reduce autofluorescence, washed, incubated for 1 h at room temperature with 1 M glycine in PBS to reduce nonspecific cross-linking, and then washed subsequently with PBS, PBS with 0.5% Triton X-100 (TX), and PBS with TX and 2% goat serum (GS). The sections were incubated overnight at 4°C with a primary antiserum diluted in PBS with TX and GS, washed, and then incubated with a secondary antiserum diluted into PBS with GS for 2 h at room temperature. All incubations were carried out in a humidified chamber. Viral antigen was detected by EGFP in a fluorescein isothiocyanate channel (38). Neurons were identified with a 1:50 dilution of mouse monoclonal antibody AP14 (10), which recognizes the MAP2b protein (5, 36) (gift from Virginia M.-Y. Lee, University of Pennsylvania, PA). Astrocytes were identified with a 1:100 dilution of a rabbit anti-cow glial fibrillary acidic protein (GFAP) (Dako Corp., Carpinteria, CA). Secondary antibodies were a 1:100 dilution of Texas red-conjugated goat anti-mouse immunoglobulin G (IgG) or anti-rabbit IgG (Jackson ImmunoResearch, West Grove, PA). Control slides were incubated in parallel with preimmune rabbit sera, and sections from mock-infected mice were incubated with secondary antibodies only. Tissue sections were sequentially washed with PBS plus TX and with PBS and mounted and visualized by fluorescence microscopy with a 40× UPlanApo oil immersion objective, with the iris diaphragm partially closed to limit the contribution of out-of-plane fluorescence, and with filter packs suitable for green fluorescence (U-MWIBA; exciter, BP460-490; beam splitter, DM505; emitter, BA515-550) and red fluorescence (U-MNG; exciter, BP530-550; beam splitter, DM570; emitter, BA590-800+). Images were acquired with a Hamamatsu Orca-1 charge-coupled device camera and Image-Pro image analysis software (Media Cybernetics, Silver Spring, MD).
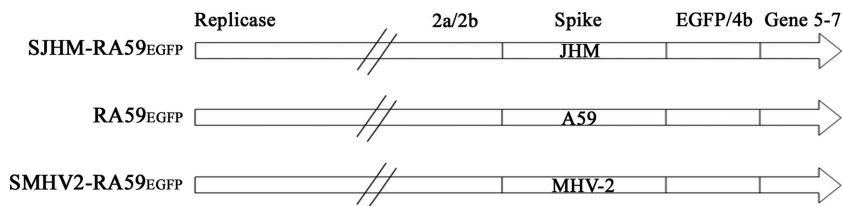
FIG. 1. EGFP-tagged isogenic recombinant viruses differ in the spike gene. A schematic diagram of the replacement of gene 4a and part of gene 4b in the MHV genome expressing EGFP. SJHM-RA59$_{EGFP}$ expresses the JHM spike gene, RA59$_{EGFP}$ expresses the A59 spike gene, and SMHV2-RA59$_{EGFP}$ expresses the MHV-2 spike gene in the background of the A59 gene. All three recombinant viruses derived are isogenic, differing only in the spike gene.

RESULTS

Comparative pathogenesis of demyelinating and nondemyelinating strains. We have compared the pathogenesis of SJHM-RA59$_{EGFP}$, RA59$_{EGFP}$, and SMHV2-RA59$_{EGFP}$, which are isogenic, except for the spike gene (Fig. 1). We used a 0.5LD$_{50}$ dose for these pathogenesis studies; for SJHM-RA59$_{EGFP}$, this dose was 5,000 PFU; for RA59$_{EGFP}$, it was 20,000; and for SMHV2-RA59$_{EGFP}$, it was 100 PFU. We infected eight mice in each group and repeated the experiment five times altogether. Out of a total of 40 mice infected for each group, 26 mice survived in the SJHM-RA59$_{EGFP}$-infected group, 30 mice survived in the RA59$_{EGFP}$-infected group, and 24 mice survived in the SMHV2-RA59$_{EGFP}$-infected group by day 30 postinfection. Brain and spinal cord sections from mice infected intracranially with SJHM-RA59$_{EGFP}$, RA59$_{EGFP}$, and SMHV2-RA59$_{EGFP}$ were stained either with H&E or Luxol fast blue and analyzed by light microscopy. No demyelination was observed in any of the mice infected with SMHV2-RA59$_{EGFP}$ (60% survival rate) (Fig. 2, upper panel), a result similar to that for its parental recombinant virus SMHV2-RA59 (previously called Penn 98-1/2) (4). In contrast, demyelination was observed in 100% of the RA59$_{EGFP}$ mice and 60% of the SJHM-RA59$_{EGFP}$ mice (more than 70% survival rate) (Fig. 2, upper panel). This confirms our previous finding that the spike gene determines the demyelination property of MHV.

In order to ensure that the nondemyelinating property of SMHV2-RA59$_{EGFP}$ is not due to its inability to replicate in the host, we carried out intracranial inoculations at a 0.5LD$_{50}$ dose for two independently isolated clones of SMHV2-RA59$_{EGFP}$ and measured virus replication in mouse brain and liver as a function of time postinfection. The kinetics of viral replication and the final titers of viruses were similar, albeit slightly lower (10-fold), for the EGFP-expressing viruses in a comparison with wild-type recombinant virus. The peak of replication was observed at day 5, a result similar to those of previous studies (4, 31) (data not shown).

Histopathological studies during acute phase of the infection revealed that all three viruses produced meningoencephalitis. Brain pathology consisted of encephalitis characterized by parenchymal lymphocytic infiltrates and microglial nodules with focal neuronophagia (Fig. 2, middle panel). The parenchymal inflammation was more severe in SJHM-RA59$_{EGFP}$-infected mouse brains than in brains infected by RA59$_{EGFP}$ and SMHV2-RA59$_{EGFP}$, and brain sections from RA59$_{EGFP}$ showed comparatively more parenchymal inflammation than did those from SMHV2-RA59$_{EGFP}$. Associated lymphocytic

meningitis was also present in all three strains (Fig. 2, lower panel). Pathogenic properties of these viruses are summarized in Table 1.

Liver pathology consisted of moderate to severe hepatitis following RA59$_{EGFP}$ and SMHV2-RA59$_{EGFP}$ infection, a result similar to those for the respective parental recombinant strains (28). The infection is characterized by multiple foci of necrosis throughout the liver (data not shown). We did not observe any liver pathology in SJHM-RA59$_{EGFP}$-virus-infected mice.

Individual strains exhibit different cellular tropism. To compare the cellular tropism of demyelinating and nondemyelinating MHV strains, we performed double-label immunofluorescence on sagittal brain sections. Mice were inoculated intracranially with a 0.5LD$_{50}$ dose of SJHM-RA59$_{EGFP}$, RA59$_{EGFP}$, and SMHV2-RA59$_{EGFP}$. Infected animals were sacrificed at days 3 and 5 postinfection, and frozen sections were made. EGFP fluorescence was used to detect viral antigen-positive cells, and immunofluorescent staining was carried out using MAP2b as a neuron-specific marker and GFAP as an astrocyte-specific marker. Sections were systematically scanned in a blinded fashion. Representative pictures of dual-color fluorescence of viral antigen plus MAP2b and viral antigen plus GFAP are shown in Fig. 3 and 4, respectively. Visual microscopic observations show that SJHM-RA59$_{EGFP}$ infects neurons more than the other two strains. On the contrary, in SJHM-RA9$_{EGFP}$-infected mice, only a very small number of viral antigen-positive cells were positive for the astrocytic marker GFAP, whereas in RA59$_{EGFP}$-infected mice, EGFP-positive cells partially overlapped with GFAP staining. It appears that there are CNS cells other than astrocytes that are infected by RA59$_{EGFP}$. More surprisingly, in SMHV2-RA59$_{EGFP}$-infected mice, EGFP-positive cells were in complete overlap with GFAP, demonstrating that most infected cells were astrocytes. Thus, SJHM-RA59$_{EGFP}$ is predominantly neuron tropic, but may be less able to infect astrocytes. RA59$_{EGFP}$ is multitropic and infects neurons as well as astrocytes and also other cell types in the CNS; SMHV2-RA59$_{EGFP}$ infects mainly astrocytes and neurons with markedly reduced efficiency. Simultaneously, to avoid a high percentage of mortality at high virus dose and produce an optimal level of viral replication that does not damage the tissue to a degree that makes microscopic observation unsuitable, we chose a 0.5LD$_{50}$ dose. However, to ensure that tropism of virus during the acute stage of infection does not depend on the dose, we also performed ex-
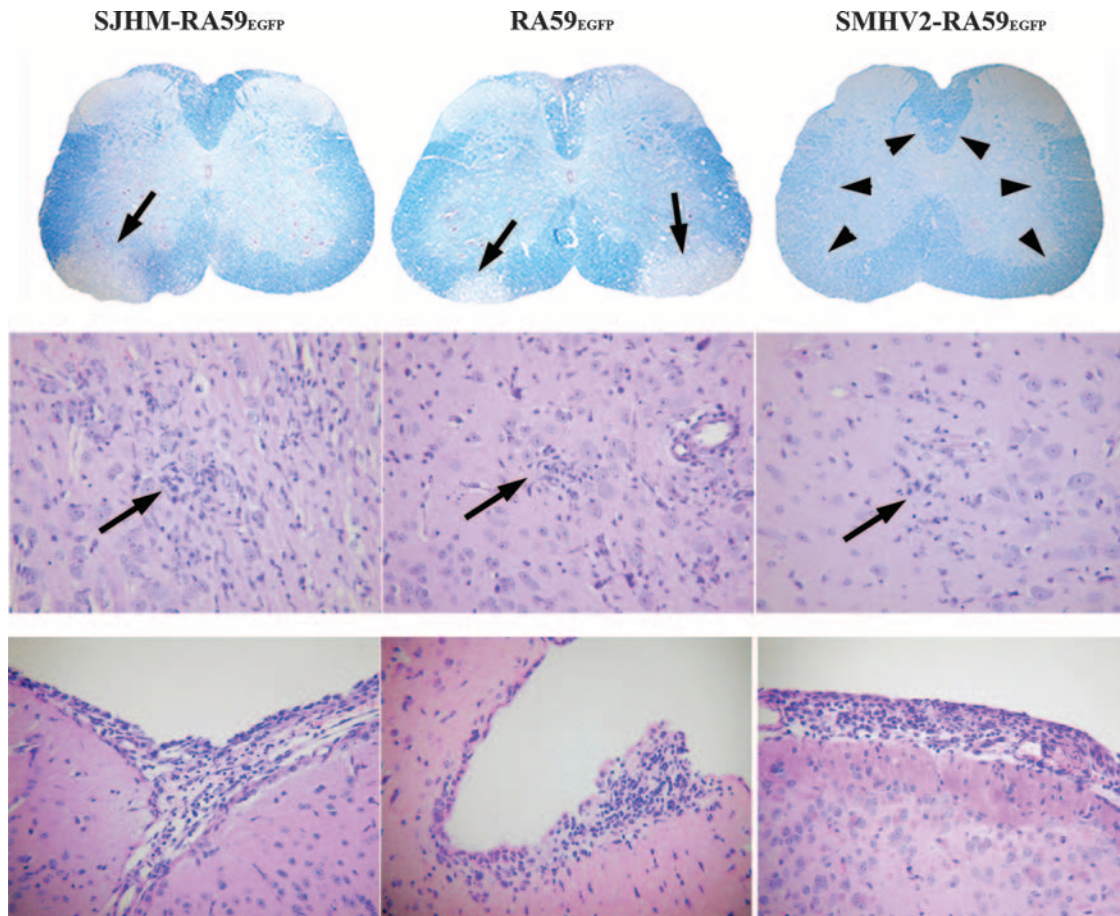
FIG. 2. CNS pathology of EGFP-expressing MHVs. The upper panel shows the observed demyelination. Luxol fast blue stained spinal cord sections of mice infected with SJHM-RA59$_{EGFP}$, RA59$_{EGFP}$, or SMHV2-RA59$_{EGFP}$, at day 30 postinfection. Thin arrows indicate a region of demyelination, and arrowheads indicate normal myelinated area of white matter. Original magnification, ×20. The middle panel shows the observed encephalitis. The microglial nodules shown are from H&E-stained basal forebrain sections of mice infected with EGFP-tagged MHVs at day 7 postinfection. Arrows indicate the microglial nodules (microglia with elongated nuclei) and lymphocytes in the vicinity of neurons in mice infected with SJHM-RA59$_{EGFP}$, RA59$_{EGFP}$, and SMHV2-RA59$_{EGFP}$. Original magnification, ×200. The lower panel shows the observed meningitis. H&E-stained sections from the basal forebrain of mice infected with EGFP-tagged MHVs at day 7 postinfection; shown are SJHM-RA59$_{EGFP}$, RA59$_{EGFP}$, and SMHV2-RA59$_{EGFP}$. In all cases, there is a brisk leptomeningeal lymphocytic inflammatory infiltrate. Original magnification, ×200.

periments which demonstrate that the cellular tropism of SMHV2-RA59$_{EGFP}$ at 500 PFU and 1,000 PFU at day 5 was similar to that at 100 PFU. We also carried out infections with 500 PFU and 1,000 PFU of SJHM-RA59$_{EGFP}$ and RA59$_{EGFP}$ and observed the same CNS cell tropism as at a higher dose, only with fewer infected cells.

Demyelinating and nondemyelinating strains differ in their viral antigen localization in gray and white matter of the spinal cord. To examine whether demyelinating and nondemy-

TABLE 1. Pathogenic properties of isogenic EGFP-expressing recombinant MHVs

Recombinant MHV strain	Status of strain for:		
	Meningitis	Encephalitis	Demyelination
SJHM-RA59$_{EGFP}$	Positive	Positive	Positive
RA59$_{EGFP}$	Positive	Positive	Positive
SMHV2-RA59$_{EGFP}$	Positive	Positive	Negative

elinating strains differ in viral antigen distribution in spinal cord gray and white matter, we collected spinal cord tissues from SJHM-RA59$_{EGFP}$-, RA59$_{EGFP}$-, and SMHV2-RA59$_{EGFP}$-infected mice at days 5 and 7 postinfection. Cross sections from several regions of all spinal cords were stained with viral anti-nucleocapsid antiserum. Ten mice were sacrificed per time point following infection by a particular viral strain. At day 5 postinfection, viral antigens were observed mainly in the gray matter of the spinal cord for all three strains, but in SJHM-RA59$_{EGFP}$- and RA59$_{EGFP}$-infected mice some viral antigen was also detected in the white matter (Fig. 5, upper panel). At day 7, most of the viral antigen in SJHM-RA59$_{EGFP}$ and RA59$_{EGFP}$ was found in white matter, whereas SMHV2-RA59$_{EGFP}$ viral antigen remained restricted mainly to gray matter, with occasional distribution to white matter (Fig. 5, middle panel). In SMHV2-RA59$_{EGFP}$-infected mice, viral antigen was observed occasionally in the white matter (3 of 60 spinal cord sections), and in some spinal cord sections of SMHV2-RA59$_{EGFP}$, viral antigen was detected at the gray-
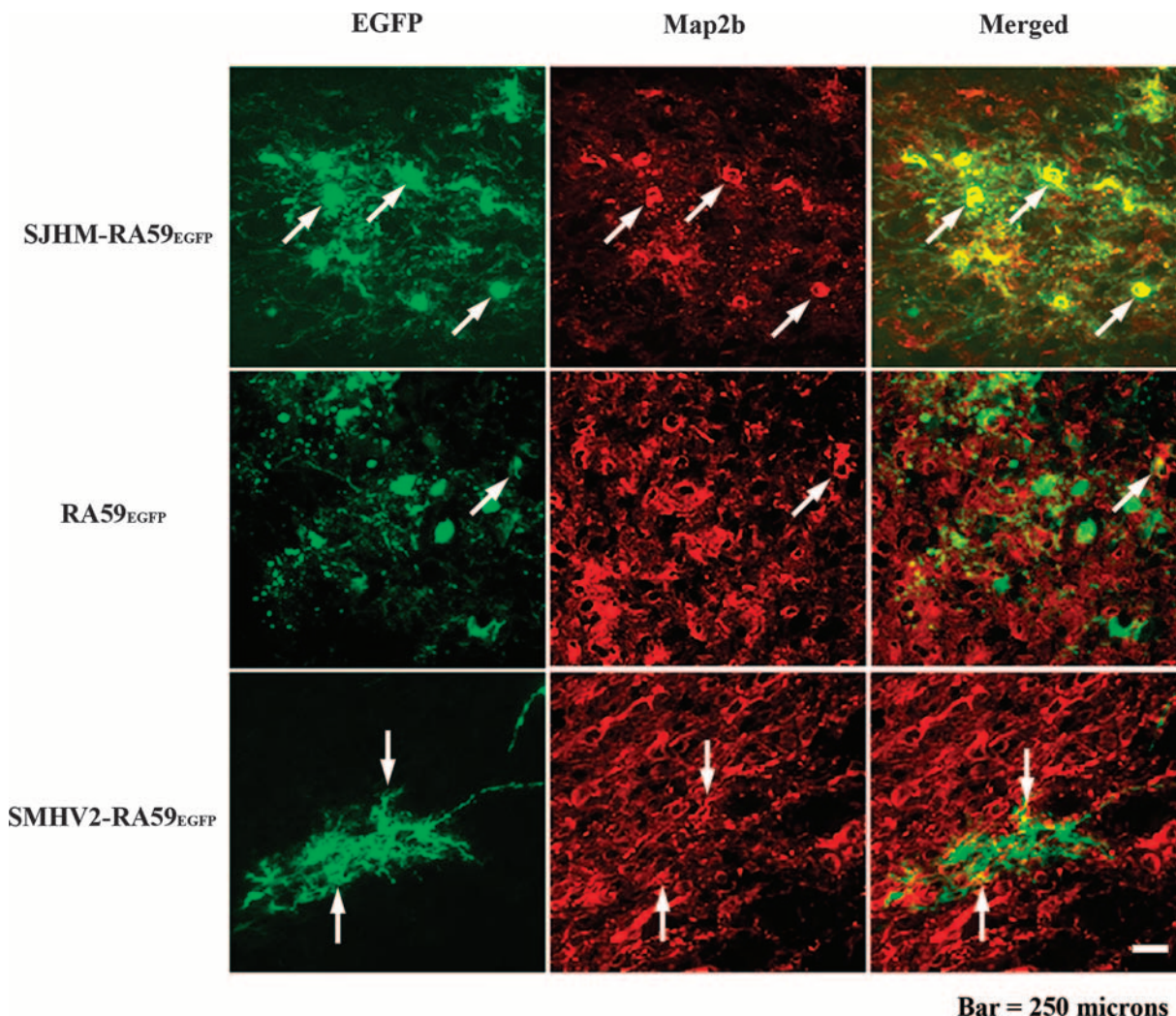
FIG. 3. Identification of EGFP MHV-infected neurons in the brain at day 5 postinfection. Mice were infected intracranially with SJHM-RA59$_{EGFP}$, RA59$_{EGFP}$, and SMHV2-RA59$_{EGFP}$. Infected mice were sacrificed at day 5 postinfection, and the brains were processed, sectioned, and then labeled with anti-MAP2b as primary antibody and with Texas red goat anti-mouse IgG as secondary antibody. EGFP fluorescence (green) was used to detect viral antigen-positive cells in the basal forebrain. Red fluorescence shows the corresponding labeling of MAP2b in neurons. Merged images show the colocalization of MAP2b- and EGFP-positive cells. Arrows identify cells double positive for viral antigen and MAP2b.

white matter junction, as shown in Fig. 5, lower panel. We repeated the experiment three times, with 10 mice in each group, and we observed similar viral antigen distributions in all three experiments.

DISCUSSION

The current studies highlight the important role of neural cell tropism of viral antigen in MHV-induced demyelination in the CNS. Localization studies showed that MHV strains that differ in their neurovirulence and abilities to demyelinate also differ in their abilities to infect particular CNS cell types. SJHM-RA59$_{EGFP}$ infects neurons with greater efficiency, and infection may spread more rapidly than RA59$_{EGFP}$, while SMHV2-RA59$_{EGFP}$ infects neurons with limited efficiency. This is consistent with previous findings (32) that the degree of neurovirulence is dependent not only on neuronal tropism but also on the number of infected neurons and the spread of the

infection through neurites. Evidence from closely related strains of neurotropic viruses, including human immunodeficiency virus, Theiler's murine encephalitis virus, and reovirus, supports the hypothesis that CNS cell tropism and spread in CNS cells play a major role in the distribution and type of CNS lesions (18, 41, 45). Studies with lymphocytic choriomeningitis virus and human immunodeficiency virus also suggest that virus strains that exhibit rapid spreading are associated with increased immune-mediated pathology (27, 44). It has previously been demonstrated that MHV spread to the spinal cord white matter occurs very rapidly, and protection from demyelination can be achieved by inhibiting this viral spread during the acute phase of infection by recruiting high numbers of MHV-specific CD8$^+$ T cells (23).

Our study highlights the diverse modes of infection that may lead to demyelination. In our study, the nondemyelinating strain is less able to infect and spread through neurons; on the
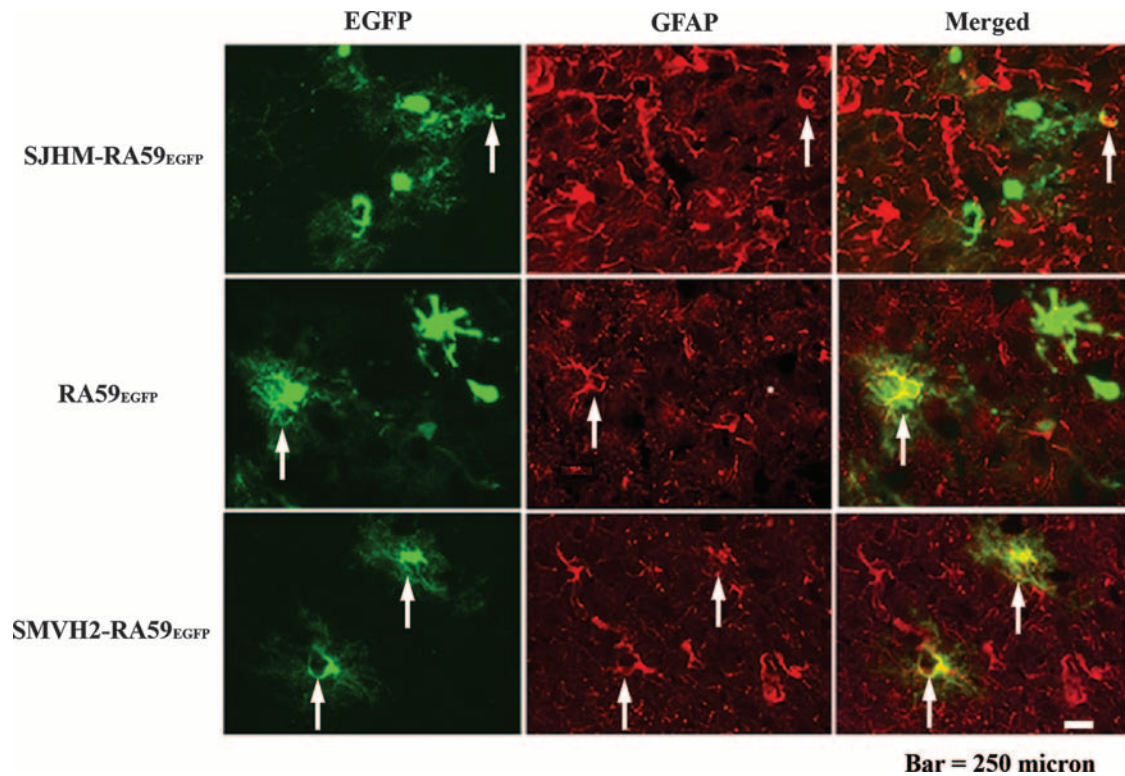
FIG. 4. Colocalization of EGFP-positive cells with astrocyte marker at day 5 postinfection. Mice were infected intracranially with SJHM-RA59$_{EGFP}$, RA59$_{EGFP}$, and SMHV2-RA59$_{EGFP}$. Infected mice were sacrificed at day 5 postinfection; brains were processed, sectioned, and then immune-labeled with anti-GFAP (astrocytic marker) antiserum, and then stained with Texas red goat anti-rabbit IgG as secondary antibodies. EGFP fluorescence was used to detect viral antigen-positive cells; red fluorescence was used to detect GFAP in astrocytes. Merged images show the colocalization of GFAP- and EGFP-positive cells. Arrows identify cells double positive for viral antigen and GFAP.

other hand, demyelinating strains are highly neuron tropic and spread rapidly through neurites. In contrast, it has previously been observed that a temperature-sensitive demyelinating mutant of JHM infects mainly nonneuronal cells (having a strong tropism specifically for astrocytes) and causes white matter lesions (11, 16). Similarly, it has previously been demonstrated that a monoclonal-antibody-selected JHM variant, a spike protein mutant, infects the glial cells predominantly in the CNS, causing subacute demyelination (8, 9). Interestingly, the neurotropic and nondemyelinating MHV3 strain, which has an in vitro tropism for neurons, ependymal cells, and meningeal cells, but not for astrocytes and oligodendrocytes, can induce an initial ependymitis, meningitis, and encephalitis in the absence of white matter lesions (40). Our in vivo data demonstrate that the highly neurovirulent strain SJHM-RA59$_{EGFP}$ has very little tropism for astrocytes. RA59$_{EGFP}$ and SMHV2-RA59$_{EGFP}$ infect astrocytes with similar efficiencies. As demyelinating and nondemyelinating strains produce similar infections in astrocytes, it appears that astrocytic infection during the acute stage alone may not determine the onset of demyelination. Our observations suggest that astrocyte tropism may be a relevant factor in persistent infection, but direct astrocytic infection alone may not be sufficient to induce demyelination.

The development of chronic demyelination involves the replication and spread of viral antigen in the spinal cord during the acute stage of infection and the persistence of viral RNA in white matter. This is substantiated by our observations on viral spread of nondemyelinating MHV in the spinal cord, where viral antigen during the acute phase of infection is restricted mainly to gray matter. In contrast, viral antigen from demyelinating strains spreads from gray to white matter during the acute stage of infection. Specifically, after intracranial infection and replication, viral antigens from the demyelinating strains SJHM-RA59$_{EGFP}$ and RA59$_{EGFP}$ are seen mostly in spinal cord gray matter at day 5 postinfection and then in white matter at day 7 postinfection. Our results establish that demyelinating and nondemyelinating strains differ in their viral antigen distribution in gray matter and white matter during acute infection. Viral persistence observed previously in SMHV2-RA59-infected mouse spinal cords during the chronic phase of infection may be due to the presence of viral RNA in gray matter (4). Viral RNA for demyelinating strains is known to persist mainly in the white matter (29). Due to lack of viral RNA persistence in the white matter, which is essential for the induction of demyelination during chronic infection, SMHV2-RA59 is unable to induce demyelination. It is possible that cell-specific viral RNA persistence is necessary for demyelination. These combined observations reinforce the importance of glial cell infection in the onset of demyelination.

It can also be argued that the spread of viral antigen from neuron to neuron and from neuron to glial cells plays a critical role in the induction of chronic-stage demyelination. Although there are no experimental data to demonstrate this argument, it can be suggested, based on our current neural cell tropism
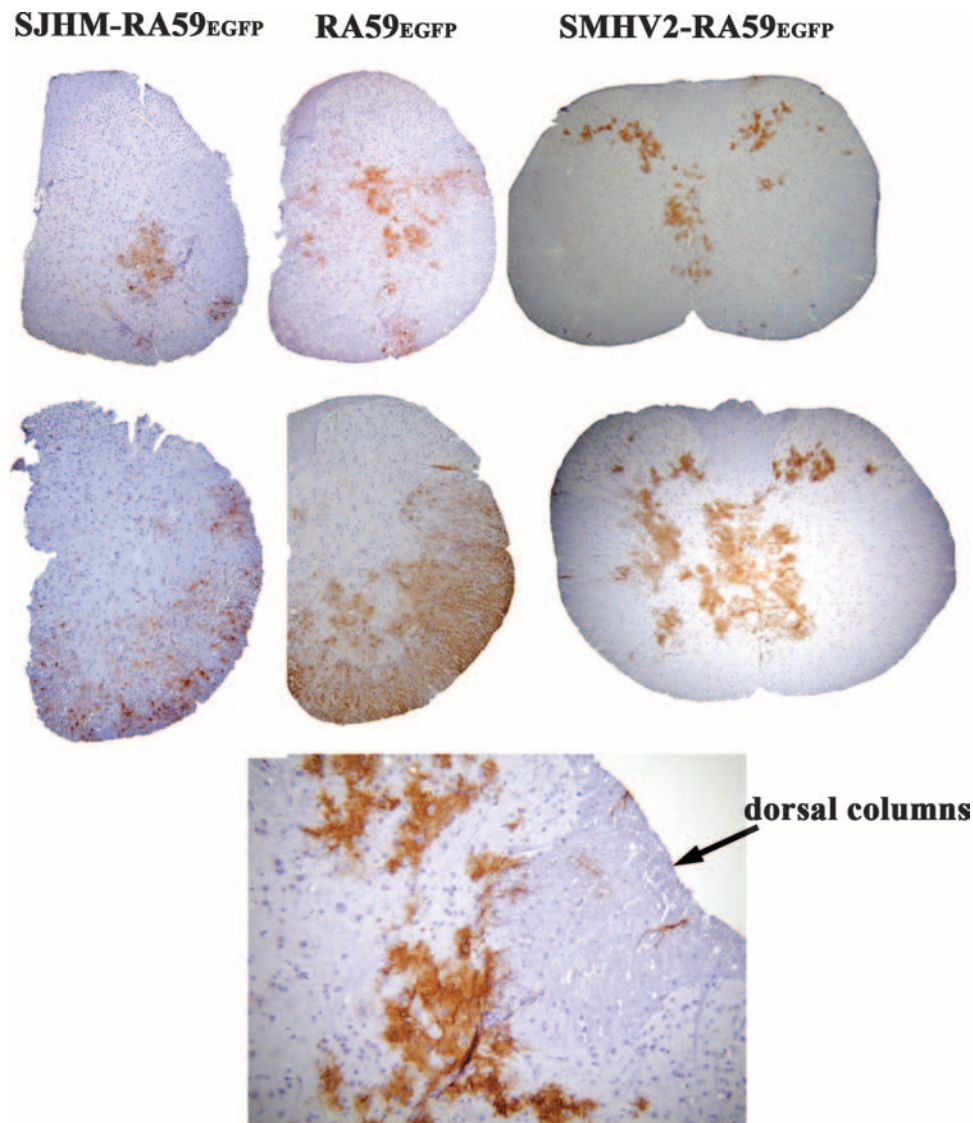
FIG. 5. Viral antigen expression in spinal cord sections of mice infected with EGFP-expressing viruses. Mice were inoculated intracranially with SJHM-RA59$_{EGFP}$, RA59$_{EGFP}$, and SMHV2-RA59$_{EGFP}$. Mice were sacrificed at days 5 and 7 postinfection, and spinal cord sections were stained with anti-nucleocapsid antiserum. Representative hemisections and complete sections of spinal cords are shown from the cervical regions of the spinal cords of mice infected on day 5 (upper panel) and day 7 (middle panel). In SMHV2-RA59$_{EGFP}$-infected mice, occasional viral antigen distribution in the white matter and gray-white matter junction is shown in the lower panel.

studies, that neuroinvasion by MHV may require entry into the nerve endings, transport to the cell body, replication in the cell body, axonal transport to the synapse, and transneuronal viral spread. Similar mechanisms of axonal transport of virus particles have been observed for the alphaherpesviruses, herpes simplex virus, and pseudorabies virus (6, 7). Furthermore, Theiler's murine encephalitis virus, a nonenveloped virus that like MHV, causes chronic demyelination in mice, is able to traffic from the axon into the surrounding myelin in the absence of cell lysis (37). Thus, by a mechanism involving transneuronal spread, MHV may gain access to synaptically linked neuronal circuits and glial cells. It is not clear, however, which type(s) of glial cells must be infected in order to promote the development of MHV-induced chronic demyelinating disease.

Our studies focused mainly on neurons and astrocytes, as they represent the majority of infected cells during the acute stage of MHV infection, but we cannot disregard oligodendrocytes. It has previously been demonstrated that MHV can infect oligodendrocytes (22), but the direct cytolytic effect of MHV on oligodendrocytes is unclear (13, 14). Direct viral infection of oligodendrocytes may contribute to MHV-induced demyelination, as observed in another human demyelinating disease, progressive multifocal leukoencephalopathy, which is caused by JC virus infection of oligodendrocytes (24, 35). Experiments are under way to optimize techniques that will facilitate detection of oligodendrocytes in MHV-infected tissues.

In summary, combined assessment of brain and spinal cord infections allows us to infer an indirect role of neuronal cell tropism in demyelination. SJHM-RA59$_{EGFP}$ and RA59$_{EGFP}$ infection can both spread from gray matter to white matter and

induce demyelination. The inability of the nondemyelinating strain of MHV, SMHV2-RA59$_{EGFP}$, to spread from gray matter to white matter cells in the spinal cord may be due to its inefficient spread through neurites. Acute-stage inflammation and chronic-stage demyelination may be two independent phenomena; however, acute-stage neuronal infection and the lack of viral spread from neuronal to glial cells are likely key elements in the induction of demyelination.

REFERENCES

1. **Allen, I., and B. Brankin.** 1993. Pathogenesis of multiple sclerosis—the immune diathesis and the role of viruses. J. Neuropathol. Exp. Neurol. **52:**95–105.
2. **Buchmeier, M. J., and T. E. Lane.** 1999. Viral-induced neurodegenerative disease. Curr. Opin. Microbiol. **2:**398–402.
3. **Das Sarma, J., L. Fu, S. T. Hingley, M. M. Lai, and E. Lavi.** 2001. Sequence analysis of the S gene of recombinant MHV-2/A59 coronaviruses reveals three candidate mutations associated with demyelination and hepatitis. J. Neurovirol. **7:**432–436.
4. **Das Sarma, J., L. Fu, J. C. Tsai, S. R. Weiss, and E. Lavi.** 2000. Demyelination determinants map to the spike glycoprotein gene of coronavirus mouse hepatitis virus. J. Virol. **74:**9206–9213.
5. **De Camilli, P., P. E. Miller, F. Navone, W. E. Theurkauf, and R. B. Vallee.** 1984. Distribution of microtubule-associated protein 2 in the nervous system of the rat studied by immunofluorescence. Neuroscience **11:**817–846.
6. **Enquist, L. W., P. J. Husak, B. W. Banfield, and G. A. Smith.** 1998. Infection and spread of alphaherpesviruses in the nervous system. Adv. Virus Res. **51:**237–347.
7. **Enquist, L. W., M. J. Tomishima, S. Gross, and G. A. Smith.** 2002. Directional spread of an alpha-herpesvirus in the nervous system. Vet. Microbiol. **86:**5–16.
8. **Fazakerley, J. K., and M. J. Buchmeier.** 1993. Pathogenesis of virus-induced demyelination. Adv. Virus Res. **42:**249–324.
9. **Fleming, J. O., M. D. Trousdale, F. A. el-Zaatari, S. A. Stohlman, and L. P. Weiner.** 1986. Pathogenicity of antigenic variants of murine coronavirus JHM selected with monoclonal antibodies. J. Virol. **58:**869–875.
10. **Geisert, E. E., Jr., H. G. Johnson, and L. I. Binder.** 1990. Expression of microtubule-associated protein 2 by reactive astrocytes. Proc. Natl. Acad. Sci. USA **87:**3967–3971.
11. **Haspel, M. V., P. W. Lampert, and M. B. Oldstone.** 1978. Temperature-sensitive mutants of mouse hepatitis virus produce a high incidence of demyelination. Proc. Natl. Acad. Sci. USA **75:**4033–4036.
12. **Houtman, J. J., and J. O. Fleming.** 1996. Pathogenesis of mouse hepatitis virus-induced demyelination. J. Neurovirol. **2:**361–376.
13. **Kalicharran, K., and S. Dales.** 1996. The murine coronavirus as a model of trafficking and assembly of viral proteins in neural tissue. Trends Microbiol. **4:**264–269.
14. **Kalicharran, K., D. Mohandas, G. Wilson, and S. Dales.** 1996. Regulation of the initiation of coronavirus JHM infection in primary oligodendrocytes and L-2 fibroblasts. Virology **225:**33–43.
15. **Knobler, R. L., M. Dubois-Dalcq, M. V. Haspel, A. P. Claysmith, P. W. Lampert, and M. B. Oldstone.** 1981. Selective localization of wild type and mutant mouse hepatitis virus (JHM strain) antigens in CNS tissue by fluorescence, light and electron microscopy. J. Neuroimmunol. **1:**81–92.
16. **Knobler, R. L., M. V. Haspel, and M. B. Oldstone.** 1981. Mouse hepatitis virus type 4 (JHM strains)-induced fatal central nervous system disease. I. Genetic control and murine neuron as the susceptible site of disease. J. Exp. Med. **153:**832–843.
17. **Knobler, R. L., P. W. Lampert, and M. B. Oldstone.** 1982. Virus persistence and recurring demyelination produced by a temperature-sensitive mutant of MHV-4. Nature **298:**279–280.
18. **Koyanagi, Y., S. Miles, R. T. Mitsuyasu, J. E. Merrill, H. V. Vinters, and I. S. Chen.** 1987. Dual infection of the central nervous system by AIDS viruses with distinct cellular tropisms. Science **236:**819–822.
19. **Lavi, E., P. S. Fishman, M. K. Highkin, and S. R. Weiss.** 1988. Limbic encephalitis after inhalation of a murine coronavirus. Lab. Investig. **58:**31–36.
20. **Lavi, E., D. H. Gilden, M. K. Highkin, and S. R. Weiss.** 1984. Persistence of mouse hepatitis virus A59 RNA in a slow virus demyelinating infection in mice as detected by in situ hybridization. J. Virol. **51:**563–566.
21. **Lavi, E., D. H. Gilden, Z. Wroblewska, L. B. Rorke, and S. R. Weiss.** 1984. Experimental demyelination produced by the A59 strain of mouse hepatitis virus. Neurology **34:**597–603.
22. **Lavi, E., A. Suzumura, M. Hirayama, M. K. Highkin, D. M. Dambach, D. H. Silberberg, and S. R. Weiss.** 1987. Coronavirus mouse hepatitis virus (MHV)-A59 causes a persistent, productive infection in primary glial cell cultures. Microb. Pathog. **3:**79–86.
23. **MacNamara, K. C., M. M. Chua, P. T. Nelson, H. Shen, and S. R. Weiss.** 2005. Increased epitope-specific CD8$^+$ T cells prevent murine coronavirus spread to the spinal cord and subsequent demyelination. J. Virol. **79:**3370–3381.
24. **Major, E. O., K. Amemiya, C. S. Tornatore, S. A. Houff, and J. R. Berger.** 1992. Pathogenesis and molecular biology of progressive multifocal leukoencephalopathy, the JC virus-induced demyelinating disease of the human brain. Clin. Microbiol. Rev. **5:**49–73.
25. **McFarlin, D. E., and H. F. McFarland.** 1982. Multiple sclerosis (first of two parts). N. Engl. J. Med. **307:**1183–1188.
26. **McFarlin, D. E., and H. F. McFarland.** 1982. Multiple sclerosis (second of two parts). N. Engl. J. Med. **307:**1246–1251.
27. **Moskophidis, D., M. Battegay, M. van den Broek, E. Laine, U. Hoffmann-Rohrer, and R. M. Zinkernagel.** 1995. Role of virus and host variables in virus persistence or immunopathological disease caused by a non-cytolytic virus. J. Gen. Virol. **76:**381–391.
28. **Navas, S., S. H. Seo, M. M. Chua, J. D. Sarma, E. Lavi, S. T. Hingley, and S. R. Weiss.** 2001. Murine coronavirus spike protein determines the ability of the virus to replicate in the liver and cause hepatitis. J. Virol. **75:**2452–2457.
29. **Perlman, S., G. Jacobsen, A. L. Olson, and A. Afifi.** 1990. Identification of the spinal cord as a major site of persistence during chronic infection with a murine coronavirus. Virology **175:**418–426.
30. **Perlman, S., N. Sun, and E. M. Barnett.** 1995. Spread of MHV-JHM from nasal cavity to white matter of spinal cord. Transneuronal movement and involvement of astrocytes. Adv. Exp. Med. Biol. **380:**73–78.
31. **Phillips, J. J., M. M. Chua, E. Lavi, and S. R. Weiss.** 1999. Pathogenesis of chimeric MHV4/MHV-A59 recombinant viruses: the murine coronavirus spike protein is a major determinant of neurovirulence. J. Virol. **73:**7752–7760.
32. **Phillips, J. J., M. M. Chua, G. F. Rall, and S. R. Weiss.** 2002. Murine coronavirus spike glycoprotein mediates degree of viral spread, inflammation, and virus-induced immunopathology in the central nervous system. Virology **301:**109–120.
33. **Qiu, Z., S. T. Hingley, G. Simmons, C. Yu, J. Das Sarma, P. Bates, and S. R. Weiss.** 2006. Endosomal proteolysis by cathepsins is necessary for murine coronavirus mouse hepatitis virus type 2 spike-mediated entry. J. Virol. **80:**5768–5776.
34. **Reed, L., and H. Muench.** 1938. A simple method of estimating fifty percent end points. Am. J. Hyg. **27:**493–497.
35. **Richardson-Burns, S. M., B. K. Kleinschmidt-DeMasters, R. L. DeBiasi, and K. L. Tyler.** 2002. Progressive multifocal leukoencephalopathy and apoptosis of infected oligodendrocytes in the central nervous system of patients with and without AIDS. Arch. Neurol. **59:**1930–1936.
36. **Riederer, B. M., E. Draberova, V. Viklicky, and P. Draber.** 1995. Changes of MAP2 phosphorylation during brain development. J. Histochem. Cytochem. **43:**1269–1284.
37. **Roussarie, J. P., C. Ruffie, J. M. Edgar, I. Griffiths, and M. Brahic.** 2007. Axon myelin transfer of a non-enveloped virus. PLoS One **2:**e1331.
38. **Sarma, J. D., E. Scheen, S. H. Seo, M. Koval, and S. R. Weiss.** 2002. Enhanced green fluorescent protein expression may be used to monitor murine coronavirus spread in vitro and in the mouse central nervous system. J. Neurovirol. **8:**381–391.
39. **Stohlman, S. A., and L. P. Weiner.** 1981. Chronic central nervous system demyelination in mice after JHM virus infection. Neurology **31:**38–44.
40. **Tardieu, M., O. Boespflug, and T. Barbe.** 1986. Selective tropism of a neurotropic coronavirus for ependymal cells, neurons, and meningeal cells. J. Virol. **60:**574–582.
41. **Weiner, H. L., M. L. Powers, and B. N. Fields.** 1980. Absolute linkage of virulence and central nervous system cell tropism of reoviruses to viral hemagglutinin. J. Infect. Dis. **141:**609–616.
42. **Weiner, L. P.** 1973. Pathogenesis of demyelination induced by a mouse hepatitis. Arch. Neurol. **28:**298–303.
43. **Weiner, L. P., R. T. Johnson, and R. M. Herndon.** 1973. Viral infections and demyelinating diseases. N. Engl. J. Med. **288:**1103–1110.
44. **Wodarz, D., and D. C. Krakauer.** 2000. Defining CTL-induced pathology: implications for HIV. Virology **274:**94–104.
45. **Zoecklein, L. J., K. D. Pavelko, J. Gamez, L. Papke, D. B. McGavern, D. R. Ure, M. K. Njenga, A. J. Johnson, S. Nakane, and M. Rodriguez.** 2003. Direct comparison of demyelinating disease induced by the Daniel's strain and BeAn strain of Theiler's murine encephalomyelitis virus. Brain Pathol. **13:**291–308.